Characterization of Highly Branched Poly(methyl methacrylate) by Solution Viscosity and Viscoelastic Spectroscopy

Peter F. W. Simon,[†,‡] Axel H. E. Müller,[*,‡] and Tadeusz Pakula[*,§]

Institut für Physikalische Chemie, Universität Mainz, Welderweg 15, D-55099 Mainz, Germany, Makromolekulare Chemie II and Bayreuther Institut für Makromolekülforschung, Universität Bayreuth, D-95440 Bayreuth, Germany, and Max-Planck Institute for Polymer Research, Postfach 3148, 55021 Mainz, Germany

Received August 24, 2000; Revised Manuscript Received November 27, 2000

ABSTRACT: Highly branched poly(methyl methacrylate) with an estimated degree of branching $\overline{DB}$ = 0.074 (i.e., 3.7 branchpoints per 100 monomer units) was prepared using self-condensing group transfer copolymerization (SCVCP) of methyl methacrylate (MMA) and 2-(2-methyl-1-triethylsiloxy-1-propenyloxy)-ethyl methacrylate (MTSHEMA) and fractionated by means of preparative SEC. The fractions were characterized in solution by SEC−viscosity coupling and in the melt by viscoelastic spectroscopy. In THF solution, a Mark−Houwink exponent of $\alpha = 0.40$ was determined for the branched polymer, which is considerably lower than that of linear PMMA ($\alpha = 0.688$). In the region between the relaxation times of the chain, τ_c, and of the segments, τ_s, of the viscoelastic spectrum of the branched polymer, both the storage and the loss moduli (log G' and log G'') are nearly equal, and the complex viscosities show a practically linear dependence on log ω with a slope of −0.54. This is attributed to a broad distribution of relaxation times and the absence of entanglements, similar to near-critical gels. The normalized chain relaxation times scale with the molecular weight with an exponent of $\alpha = 2.61$, which again is considerably lower than the value for the linear case ($\alpha = 3.39$).

Introduction

Recently, branched polymers have experienced increasing interest. In addition to star- and comb-shaped macromolecules, hyperbranched polymers are attractive because they combine some properties of dendrimers, such as a self-similar structure and an exponentially increasing number of end groups, with the advantage of facile and inexpensive preparation. These polymers usually exhibit a very broad molecular weight distribution, which makes their characterization more demanding. This might also constitute a limiting factor for their use in applications characteristic of dendrimers.

Fréchet et al.[1] prepared hyperbranched vinyl polymers using a technique called self-condensing vinyl polymerization (SCVP) of initiator-monomers having the general structure AB*, where A stands for a double bond and B* stands for an initiating group. Thus, these species combine features of an initiator and a monomer and have therefore been named "inimers".[2] This approach has been applied to various types of living polymerization, i.e., cationic,[1,3] ATRP,[4] nitroxide-mediated radical polymerization,[5] and even ring-opening polymerization.[6] We have used group transfer polymerization (GTP) of the inimer 2-(2-methyl-1-triethylsiloxy-1-propenyloxy)ethyl methacrylate (MTSHEMA, **1**), where the silylketene acetal group can be activated by nucleophilic catalysts to initiate GTP.[7−10]

Self-condensing vinyl copolymerization (SCVCP) of AB* monomers with conventional monomers, M, leads to highly branched polymers, allowing for control of the molecular weight distribution (MWD) and degree of branching.[4,6,11−16] Alternatively, these copolymers can

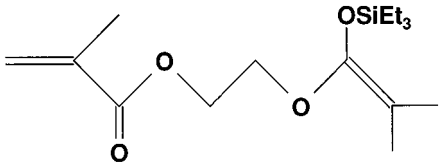

1

be prepared via SCVP of "macroinimers",[17] i.e., heterotelechelic macromolecules including both an initiating and a polymerizable moiety. Both processes permit control of the molecular weight distribution as well as the degree of branching, $\overline{DB}$, through the ratio of the initial concentrations of the monomer and inimer, $\gamma = [M]_0/[I]_0$.

Depending on the chemical nature of comonomers, different types of functional groups can be incorporated into the polymer. Because the number of linear units is increased, the *DB* of the copolymers becomes lower than that of SCVP homopolymers. However, the effect on solution properties such as intrinsic viscosity and radius of gyration should be small, because branched polymers above a limiting molecular weight are self-similar objects.[18] Therefore, copolycondensation or copolymerization is an economic approach to obtaining highly branched polymers, especially when control on rheology is an aim.

Experimental data on the solution properties and melt rheology of highly branched structures are scarcely found in the literature. This might be because of the broad molecular weight distributions of the hyperbranched polymers, which makes it difficult to obtain reliable data. Nunez et al.[19] investigated the rheology of semidilute solutions of hyperbranched 2,2-dimethylpropionic acid and found that they exhibit Newtonian behavior, indicating the absence of entanglements. Sendijarevic and McHugh[20] compared the melt rheology

* Author to whom correspondence should be addressed. E-mail: axel.mueller@uni-bayreuth.de.
† Universität Mainz.
‡ Universität Bayreuth.
§ Max-Planck Institute for Polymer Research.

10.1021/ma0014766 CCC: $20.00
Published on Web 02/15/2001

of these hyperbranched polymers with that of poly(propylenime) dendrimers and found Newtonian behavior in both cases, as well as no intermolecular entanglement formation.

Jackson et al.[21] investigated the properties of dilute solutions by comparing the intrinsic viscosity and radius of gyration of fractionated and unfractionated moderately branched poly(methyl methacrylate)s, prepared by free-radical copolymerization of methyl methacrylate with ethylene glycol dimethacrylate using multi-detector size-exclusion chromatography (SEC). The authors found the *z*-average radius of gyration of these polymers to be insensitive to branching and detected some evidence for increased polydispersity after SEC separation at higher molecular weights.

The viscoelastic or rheological behavior of polymers in melts is strongly related to the size of the macromolecules and to their topology. For melts of linear monodisperse chains, the viscoelastic spectra provide information about both segmental and chain relaxation times, which, through known scaling dependences, allow for a determination of the macromolecular sizes of test samples. Even a determination of molecular weight distributions has been attempted using the viscoelastic behavior of linear polymers. The situation is more complicated for macromolecules with other-than-linear topologies for which the scaling dependences are different and in many cases not well-known or tested. Especially difficult seems to be systems in which both the sizes and the topologies of molecules are not precisely known and can vary in an undefined way. This seems to be the case for the broad distribution of sizes of highly branched, but poorly defined, molecular topologies. The determination of the molecular weight distribution of branched polymers is still a challenging endeavor. Because of the branched nature of the samples, the hydrodynamic volume for a given molecular weight differs significantly from that of a linear sample. Therefore, the use of a linear calibration curve in SEC leads to erroneous results. This problem can be overcome by the use of mass-sensitive on-line detectors such as a multi-angle laser light photometer (MALLS)[22,23] or a viscosity detector using the universal calibration (UNICAL) technique.[24] However, this technique has some shortcomings. Universal calibration is based on empirical results, whereas the theoretical base of this technique is very poorly understood.

In this paper, we present viscosity and rheological properties of melts of the highly branched methacrylates prepared by the SCVCP of the inimer **1** with methyl methacrylate (MMA). To overcome the drawback of a broad molecular weight distribution, we used preparative size-exclusion chromatography in order to fractionate the branched polymer into a number of samples with low polydispersity. The molecular weight distributions of these fractions were determined using multi-detector size-exclusion chromatography with on-line viscosity and light scattering detection. This technique leads to absolute molecular weights, as well as data on solution properties. However, it should be stressed that SEC fractionates polymers according to their hydrodynamic volume. Consequently, these "narrow" fractions can consist of a mixture between polymers with different *DB* and *M* values exhibiting the same hydrodynamic volume.

Experimental Part

Materials. Tetrahydrofuran (THF, BASF) was fractionated over a 1-m column and dried over potassium. After being degassed, the solvent was stirred over sodium/potassium alloy and distilled in vacuo prior to use. Methyl methacrylate (MMA, Röhm GmbH) was fractionated from CaH_2 over a 1-m column filled with Sulzer packing at 45 mbar. After being degassed, the distillate was stirred over CaH_2, degassed, and distilled under high vacuum. Ethyleneglycol dimethacrylate (Aldrich), dibenzoylperoxide (Aldrich), chlorotris(triphenylphosphine) rhodium(I) (Fluka) and triethylsilane (Fluka) were used without prior purification. Tetrabutylammonium bibenzoate (TBABB) was prepared according to the known procedure.[25] 2-(2-Methyl-1-triethylsiloxy-1-propenyloxy)ethyl methacrylate (MTSHEMA) was prepared according to ref 9, in a procedure analogous to that described by Ojima and Kumagai.[26]

Polymerizations. The copolymerization of MTSHEMA with MMA was performed at room temperature by the following procedure. Under inert conditions, a mixture of 2.4 g (7.6 mmol) of MTSHEMA and 19.7 g (197 mmol) of MMA was prepared in 200 mL of THF (comonomer ratio γ = [MMA]/[MTSHEMA] = 26). The polymerization was started by addition of 1 mL of a solution of TBABB in THF (1.9 μmol) under vigorous stirring. After 20 min, the reaction was quenched with a mixture of methanol and acetic acid. The solvent was partially evaporated, and the polymer was recovered by precipitation with methanol and dried for 48 h at 40 °C in vacuo.

Linear PMMA samples with various molecular weights were prepared by conventional radical polymerization of methyl methacrylate in ethyl acetate and mixed in order to obtain a sample with a broad molecular weight distribution. These polymers were used for comparison in the solution viscosity studies. The linear PMMA samples used in viscoelastic spectroscopy are commercial standards prepared by anionic and group transfer polymerizations (PSS and PL).

Typically, PMMA samples prepared by GTP as well as by free radical polymerization have comparable, predominately syndiotactic, tacticities.[27,28] Thus, we do not expect an effect of tacticity when branched polymers made by GTP are compared with linear ones made by radical polymerization.

Preparative SEC. Preparative SEC was performed at room temperature in THF using 10-μm PL-gel columns (500 Å and mixed bed in series, 600 mm × 25 mm each) at a flow rate of 8 mL/min. Samples were injected manually using a Rheodyne 7125 high-pressure valve at a typical concentration of 100 g/L (loop size = 1 mL). A Bischoff RI 8110 refractive index detector (λ = 950 nm) was used to determine the concentration. After every 7 mL, a new fraction was taken using an ISCO model 328 fraction collector. The fractions were evaporated, redissolved in benzene, and freeze-dried.

SEC Characterization. SEC measurements were performed at room temperature in THF using 5μ PSS SDV gel columns (10^3, 10^5, and 10^6 Å; 30 cm each; Polymer Standards Service, Mainz, Germany) at a flow rate of 0.5 mL/min. A Viskotek H 502B viscosity detector (operating at 30 °C), a Shodex RI-71 refractive index detector, a DAWN DSP F multi-angle laser light scattering photometer (λ_0 = 632.8 nm; scattering angles from 35.4° to 144.6° were evaluated), and an Applied Biosystems 1000S UV diode array detector were used. The refractive index increment, d*n*/d*c*, was determined using an NFT Scan-Ref interferometer (Nanofilm Technology, Göttingen, Germany) attached to SEC columns, operating at a laser wavelength of λ_0 = 632.8 nm. Raw data were processed using PSS-WinGPC V4.02 and NFT V2.0c software.

Differential Scanning Calorimetry (DSC) was performed on a Mettler-Toledo DSC 30 apparatus at 10 K/min.

Viscoelastic Spectroscopy. Dynamic mechanical measurements were performed using a Rheometric Scientific ARES mechanical spectrometer. Shear deformation was applied under conditions of controlled deformation amplitude, always within the range of linear viscoelastic response of the studied samples. Frequency dependences of the storage (G') and loss (G'') shear moduli were measured at various temper-

Scheme 1. General Route to Highly Branched Poly(methyl methacrylate) via Self-Condensing Vinyl Copolymerization

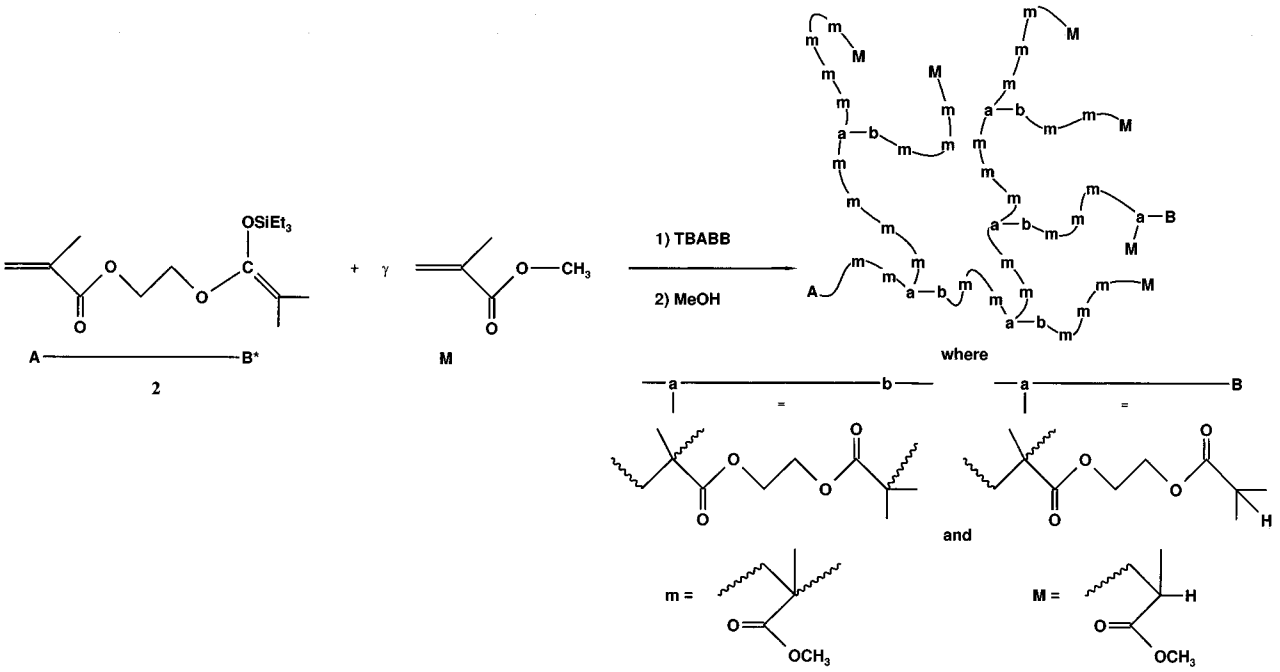

atures. A geometry of parallel plates was used below 180 °C, with plate diameters of 6 mm, whereas at higher temperatures, the measurements were performed in a cone−plate geometry with a diameter of 25 mm. In the case of the plate−plate geometry, the gap between plates (sample thickness) was about 1 mm. Experiments were performed under a dry nitrogen atmosphere. The frequency dependences of G' and G'' measured within the frequency range of 0.1−100 rad/s at various temperatures were used to construct master curves representing a broad-range frequency dependence of these quantities. Only shifts along the frequency scale were performed. This procedure provided a temperature dependence of shift factors ($\log a_T$ vs T). The low-frequency range of the master dependence of G'' (with $G'' \approx \varpi$, indicating the Newtonian-flow range) was used to determine the zero-shear viscosity at the reference temperature ($\eta_0(T_{ref}) = G''/\varpi$). Viscosity values related to other temperatures were determined via $\eta_0(T) = \eta_0(T_{ref}) + \log a_T$. The relaxation time corresponding to the transition between the Newtonian-flow range at low frequencies and the glassy range at high frequencies at the reference temperature was determined from $\tau(T_{ref}) = 1/\varpi_c$, where ϖ_c is the frequency at which the G' and G'' curves cross each other. In cases for which no clear crossing of G' and G'' at low frequencies was observed, the terminal relaxation time was determined from the crossing point of the $\log G'$ and $\log G''$ vs $\log \omega$ lines extrapolated from the lower-frequency range. Relaxation times at other temperatures are given by $\tau(T) = \tau(T_{ref}) + \log a_T$. Samples of both fractions of the hyperbranched polymers and of the melts of monodisperse linear polymers were characterized in the above-described way. The linear polymer samples are considered as a reference and test of the characterization method.

Results and Discussion

Synthesis of Highly Branched Poly(methyl methacrylate). The general synthetic route of self-condensing group transfer copolymerization is outlined in Scheme 1. Details can be found elsewhere.[16,29] The curved lines represent polymer chains and TBABB denotes the catalyst tetrabutylammonium bibenzoate.

It is well-known that GTP catalyzed by oxyanions offers the possibility for the performance of controlled polymerization of methacrylates at room temperature.[30,31] Although the concentration of active centers in self-condensing group transfer copolymerization (SCVGTP)[9] is about 1 order of magnitude higher than that in conventional GTP, no termination by backbiting[32] was detected. As a consequence, SCVGTP offers a facile synthetic route to hyperbranched methacrylates, even in larger amounts.

The low concentration of branchpoints in the polymer does not permit the determination of the degree of branching, *DB*, of the copolymer directly by spectroscopic methods. With the assumption of equal rate constants for copolymerization steps, *DB* can be expressed as a function of the comonomer ratio $\gamma = [M]_0/[I]_0$, where $[M]_0$ and $[I]_0$ represent the initial concentrations of momomer and inimer, respectively. In the present case, $\gamma = 26$, theory[12] predicts

$$\overline{DB} \approx \frac{2}{\gamma + 1} = 0.074$$

Because $\overline{DB}$ is defined as

$$\overline{DB} = \frac{2(\text{number of branched units})}{\text{total number of units} - 1}$$

we calculated a fraction of branched units $f_B = \overline{DB}/2 \approx 0.037$, i.e., we expect 37 branchpoints in 1000 monomer units. Because these values are calculated based on the assumption of equal rate constants for copolymerization, they represent a rough estimate. Recent theoretical calculations[11] show that, for nonequal rate constants, the degree of branching can be lower.

Solution Properties. In principle, SEC characterization of hyperbranched polymers gives reasonable results if some basic features are fulfilled. For a given molecular weight, a branched polymer exhibits a more densely packed structure than a linear one. That means that calibration curves established by the use of linear standards will lead to erroneous results. Universal calibration (UNICAL)[24,33] with application of an on-line

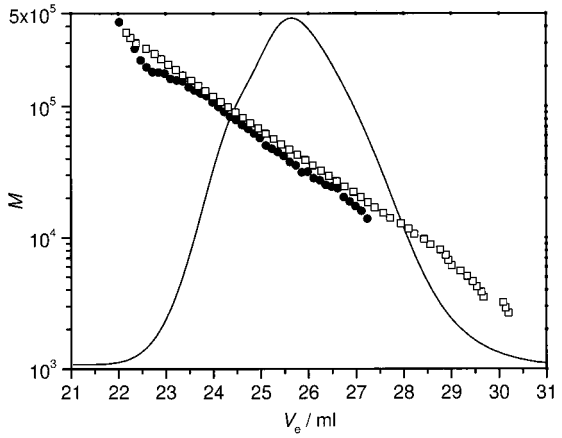

Figure 1. SEC traces and calibration curves of highly branched PMMA. (—) RI signal; calibration curves obtained by (●) MALLS and (□) UNICAL.

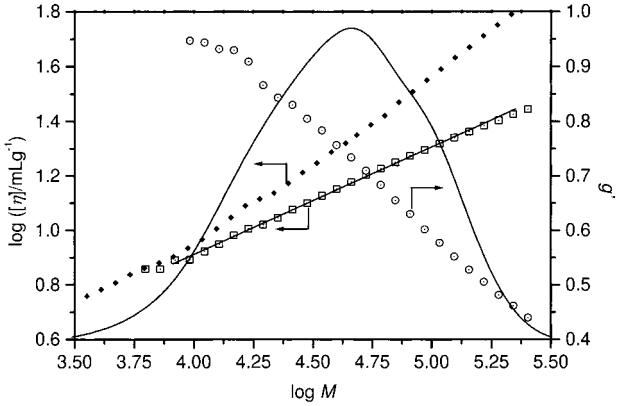

Figure 2. Mark−Houwink plot of highly branched PMMA obtained from the feed polymer. (—) RI signal; (⊡) intrinsic viscosity of feed; (◆) intrinsic viscosity of linear PMMA; (⊙) contraction factor, g'.

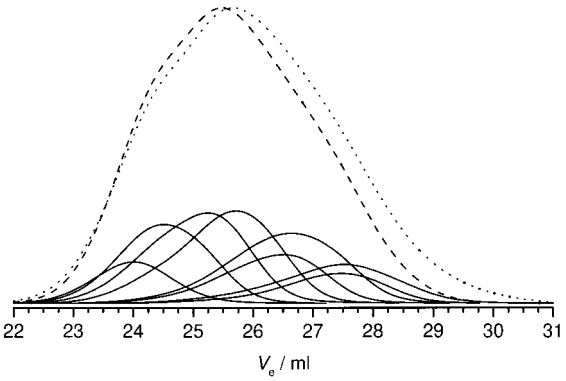

Figure 3. Separation of feed polymer into fractions by preparative SEC. (—) RI signal of fractions; (– – –) accumulated RI signal; (· · ·) RI signal of feed polymer.

viscosity detector and on-line multi-angle laser light scattering (MALLS)[22,23] present the possibility of determining absolute molecular weights and solution properties.[18] Furthermore, because of the purely statistical nature of the polymerization process, hyperbranched copolymers exhibit a rather high polydispersity with respect to the molecular weights and the distribution of the branchpoints in the polymer. At this point, it should be stressed that the latter nonuniformity is not reflected by the degree of branching, because this parameter deals only with the *number* but not with the *location* of the branchpoints in a polymer. Consequently, two macromolecules exhibiting an equal $\overline{DB}$ value could differ in their architectures.[34,35] This nonuniformity makes it questionable whether all SEC slices are monodisperse with respect to the molecular weight. To determine whether a size-exclusion separation mechanism is still operative in this case, it is necessary to cross-check SEC results with a different technique. Consequently, a hyperbranched poly(methyl methacrylate) sample was fractionated by preparative SEC, which, in any case, decreases the polydispersity with respect to the hydrodynamic volume. The SEC traces of the unfractionated polymer (feed) with calibration curves established independently by UNICAL and MALLS are shown in Figure 1. The agreement of the molecular weight averages is reasonable, although the UNICAL calibration curve is somewhat shifted to higher molecular weights. This deviation can be attributed to the low sensitivity of MALLS for small molecules (especially for the low refractive index increment, $dn/dc = 0.088 \pm 0.001$ mL/g), which causes a broader error range, or to a systematic error in UNICAL, where the principle is based on empirical evidence (vide supra).

From the measured intrinsic viscosities and the absolute molecular weights obtained from UNICAL, a Mark−Houwink plot was established for the unfractionated polymer (Figure 2). The low value of the Mark−Houwink exponent $\alpha = 0.395$, as compared to linear PMMA ($\alpha = 0.688$),[36,37] undoubtedly shows a densely packed structure resulting from the branched topology. Contraction factors,[38] $g' = [\eta]_{br}/[\eta]_{lin}$, were calculated from the Mark−Houwink plots and are given in Figure 2. It becomes clear that the relative density of the hyperbranched polymer increases with molecular weight. Unfortunately, it was not possible to determine the radius of gyration because of its small value ($R_g < 20$ nm).

The separation of the feed into the different fractions is demonstrated in Figure 3. Solid lines represent the weighted RI signals of each fraction. For a given elution volume, the sum of all signals should be equal to the RI signal of the feed polymer, which is true in Figure 3 within the experimental error. The deviation at high volumes can be explained by the fact that no fractions were collected for $V_e > 29$ mL.

Each of the eight fractions collected was characterized separately by the SEC coupling techniques described above. For fractions 2−7, it was possible to establish UNICAL and MALLS calibration curves. As shown in Figures 4 and 5, these curves are in good agreement with the results of Figure 1. The molecular weight averages obtained by UNICAL and MALLS are given in Table 1. Again, the light scattering results, especially for fractions of lower molecular weight, suffer from the low refractive index increment of the polymer, which makes the calibration curve quite noisy.

In analogy to Figure 2, Mark−Houwink plots for the different fractions were established using the absolute molecular weight obtained by UNICAL (Figure 4) and the measured intrinsic viscosities in each slice.

It can be seen from Figure 6 that, for all of the fractionated samples, the Mark−Houwink curves are nearly identical. However, the Mark−Houwink exponents, α, in Table 1 obtained by SEC−VISC of the fractionated samples are significantly lower than those determined for the feed polymer. This can be attributed to an artifact due to the axial dispersion of these narrowly distributed fractions. A similar observation

Table 1. Characterization of Branched PMMA and of Fractions in THF Solution and in the Melt

		DSC	SEC−VISC (UNICAL)					SEC−MALLS		viscoelastic spectroscopy		
fraction number	symbol	T_g (°C)	$10^4 \times M_w$	M_w/M_n	$10^4 \times M_\eta$	$[\eta]$ (mL g^{-1})	α	$10^4 \times M_w$	M_w/M_n	η_0 (MPa s)	τ_s (ms)	τ_c (s)
feed		114.5	5.52	2.05	4.54	14.94	0.402	5.80	1.84	30.5	5.59	92.16
2	□	−	12.06	1.19	11.34	22.86	0.283	15.05	1.12	20.8	1.09	160
3	○	90.6	9.64	1.22	8.97	19.56	0.320	10.09	1.04	5.71	1.10	40.8
4	△	78.6	7.20	1.25	6.65	18.02	0.329	7.09	1.15	1.68	2.93	65.4
5	▽	88.2	5.58	1.30	5.06	16.12	0.333	5.74	1.26	1.17	0.95	20.1
6	◇	90.7	3.52	1.34	3.24	14.00	0.379	4.42	1.28	0.79	0.94	5.01
7	+	83.5	3.26	1.33	2.98	12.95	0.369	3.05	1.16	0.85	0.95	1.94
8	×	90.2	2.18	1.32	1.98	10.87	0.402	2.46	1.12	0.30	0.61	0.6
9	*	85.8	2.00	1.40	1.80	11.60	0.417	−	−	0.26	0.61	0.47

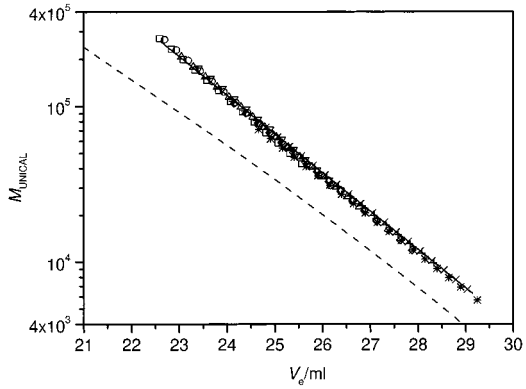

Figure 4. UNICAL calibration curve for the various fractions and comparison with feed (—). Open symbols, cf. Table 1; (− − −) linear PMMA.

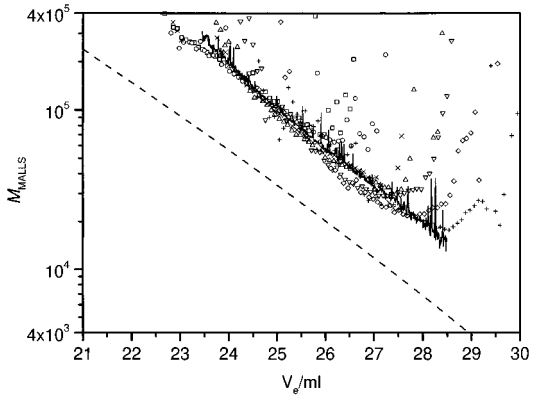

Figure 5. MALLS calibration curve for the various fractions and comparison with feed (—). Open symbols, cf. Table 1; (− − −) linear PMMA.

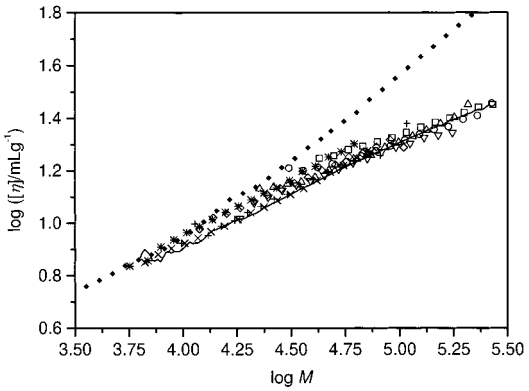

Figure 6. Mark−Houwink plot for the various fractions of highly branched PMMA (for symbols, see Table 1). (—) unfractionated feed polymer; (◆) linear PMMA.

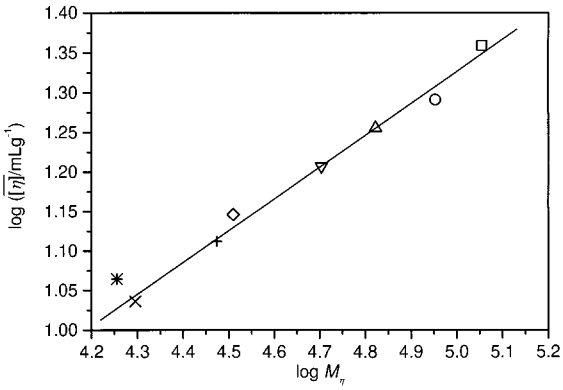

Figure 7. Mark−Houwink plot obtained from intrinsic viscosities of each fraction of hyperbranched PMMA (for symbols, see Table 1).

was made for the R_g-M dependence obtained by SEC−MALLS.[22]

To cross-check the latter value, a Mark−Houwink plot was constructed from the average intrinsic viscosities, $[\bar{\eta}]$, of each fraction and the viscosity-average molecular weight, M_η (Figure 7). This differs from Figure 4, which shows the intrinsic viscosities and the molecular weights *for each SEC slice* of the unfractionated polymer.

A linear fit of the data in Figure 7 results in a slope of $\alpha = 0.402 \pm 0.017$, which is in excellent agreement with the value determined in Figure 2.

In conclusion, we showed that, using SEC−MALLS and SEC−UNICAL, absolute molecular weight averages of hyperbranched polymers can be obtained. Furthermore, viscosity detection enables determinations of the Mark−Houwink exponent of the sample and of the contraction factors by comparison with a suitable linear standard. The hyperbranched polymer was fractionated using preparative SEC. No differences in solution properties could be detected between the SEC slices of the feed polymer and the average values of the different fractions, indicating that the separation is attributable only to differences in hydrodynamic volume and not to polymer structure or molecular weight alone.

Melt Properties. Typical viscoelastic results for a melt of linear PMMA are shown in Figure 8. The frequency dependences of G' and G'' are presented as master curves superimposed on the frequency sweeps measured at various temperatures. Temperature dependences of the shift factors were, for all samples (linear and branched), in a good agreement with the WLF relation

$$\log(a_T) = C_1(T - T_{ref})/[C_2 + (T - T_{ref})]$$

with the parameters $C_1 \approx 8.2 \pm 0.3$ and $C_2 \approx 85 \pm 5$ °C at $T_{ref} = 130$ °C. For the linear polymer melts, the dependences in Figure 8 indicate two easily distinguish-

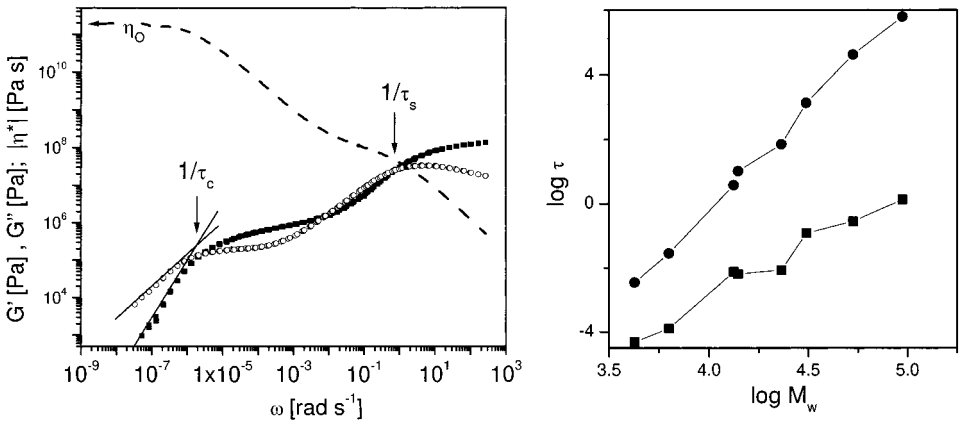

Figure 8. (a) Storage and loss moduli, G' (■) and G'' (○), respectively, and melt viscosity (− − −) of linear PMMA ($M_w = 94\,200$) as a function of shear frequency at a reference temperature of 130 °C. (b) Dependences of the chain, τ_c (●), and segmental, τ_s (■), relaxation times on the molecular weight for all linear PMMA samples.

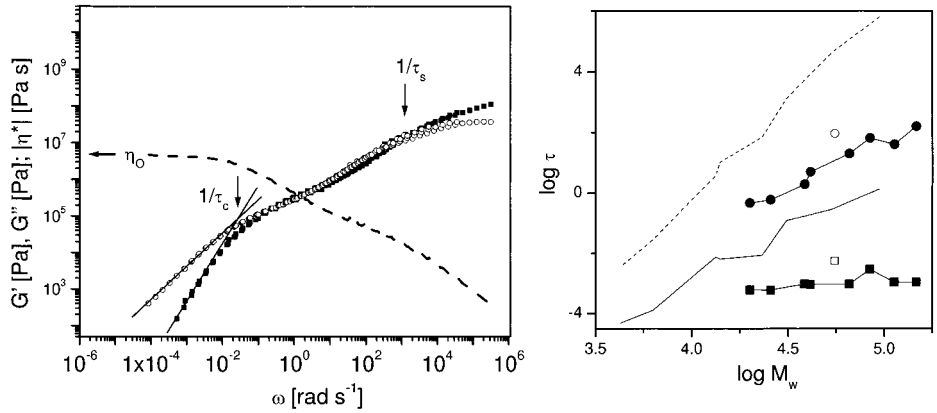

Figure 9. (a) Storage and loss moduli, G' (■) and G'' (○), respectively, and melt viscosity (− − −) of fraction 3 of highly branched PMMA ($M_w = 96\,000$) as a function of shear frequency at a reference temperature of 130 °C. (b) Dependences of the chain, τ_c (●), and segmental, τ_s (■), relaxation times on the molecular weight for all fractions; the corresponding relaxation times of the feed polymer, τ_c (○) and τ_s (□), are included for reference. Corresponding dependencies for linear PMMA (from Figure 8b) are shown by dashed and solid lines.

Table 2. Characterization of Linear PMMA by Viscoelastic Spectroscopy

sample	$10^4 \times M_W$	T_g (°C)	τ_s (s)	τ_c (s)	τ_c/τ_s	η_0 (MPa s)
L1	9.42	130.8	1.355	626,600	462435	195,000
L2	5.32	–	0.2856	42,600	149159	17,400
L3	3.10	121.49	0.122	1,359	11139	5.6
L4	2.32	116.86	0.0086	71.8	8348	8.7
L5	2.05	130.5	1.509	3240	2147	–
L6	1.40	117.5	0.0065	10.47	1610	1.45
L7	1.33	110.6	0.0075	3.83	510	0.926
L8	0.63	94.84	1.29×10^{-4}	0.0285	220	0.065
L9	0.42	96.81	4.8×10^{-5}	0.00353	73	0.017

able relaxation processes: (1) segmental relaxation at high frequencies, which separates the glassy state of the polymer from the state with local segmental mobility, and (2) chain relaxation at low frequencies, which separates the rubbery plateau corresponding to the frequency range of internal relaxations of entangled chains from the chain-flow range. Both processes are localized around the frequencies where G' and G'' cross each other, as indicated in Figure 8a by arrows. For the low-frequency relaxation, the relaxation time can alternatively be determined as the intersection of the G' and G'' dependences (indicated by the solid straight lines) extrapolated from the low-frequency range where they exhibit a characteristic behavior when the polymer flows. The relaxation times for the two processes were determined for samples with linear chains of various molecular weights (see Table 2) and are shown in Figure 8b. Some fluctuations in the segmental relaxation times are caused by differences in glass transition temperatures (cf. Table 2). These differences might be due to different tacticities of the polymers, which have not been characterized but should be quite similar (vide supra). To separate this effect from the macromolecular relaxation rates, only ratios of the chain and segmental relaxation times are considered further. The frequency dependence of the complex viscosity related to the behavior of the melt of the linear polymer is shown in Figure 8a as a dashed line. As with the G' and G'' dependences for this polymer, this dependence can be considered as consisting of four different ranges, each of which can be characterized by means of an ω^α dependence with the characteristic exponent α_{vs}: (1) the low-frequency ($\omega < 1/\tau_c$) plateau range where $|\eta^*| \approx \eta_0\omega^0$, indicating Newtonian flow with the zero-shear viscosity η_0; (2) the range of relaxation of entangled chains where $-0.8 < \alpha_{vs} < -0.7$ for the long PMMA

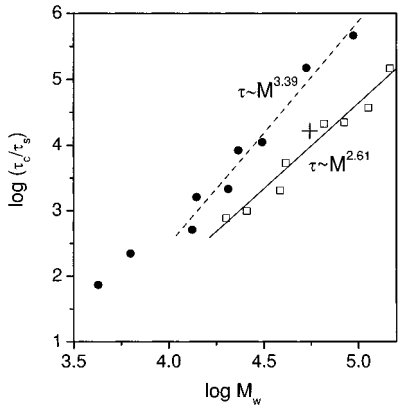

Figure 10. Molecular weight dependences of the normalized chain relaxation time, τ_c/τ_s, for linear polymers (□), branched fractions (●), and branched feed polymer (+).

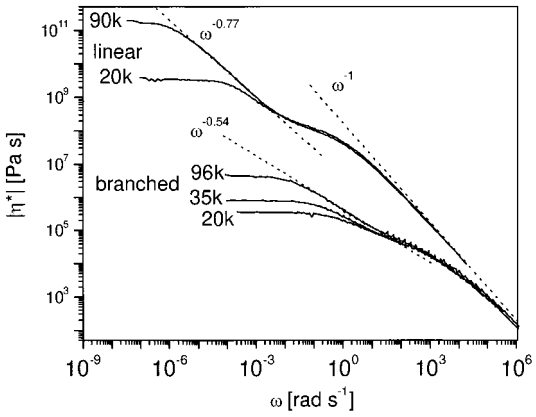

Figure 11. Frequency dependences of the complex viscosity η^* for melts of linear and branched PMMA with different M_w values.

chains; (3) the segmental local flow and the local Rouse-like relaxation of chains with $\alpha_{vs} = -0.33$; and finally, (4) the glassy range where the exponent will approach the value $\alpha_{vs} = -1$ for $\omega \gg 1/\tau_s$.

Figure 9a shows the characteristics of the viscoelastic properties determined for a single fraction of the branched polymer. As for the linear chains, two relaxations can be distinguished here, but they are much less distinctly separated each from the other and both have a considerably broader distribution of relaxation times. Nevertheless, the four frequency ranges can also be recognized here, in the behavior of both the moduli and the viscosity. The flow regime at low frequencies, $\omega < 1/\tau_c$, is clearly seen and allows for a determination of η_0 (see Table 1). The segmental and polymer relaxation times were determined as the intersection point of G' and G'' at high frequencies and as the intersection point of linear extrapolations of log G' and log G'' vs log ω in the distinctly seen terminal-flow range at low frequencies, respectively. The results for the eight fractions (Table 1) are shown in Figure 9b as a function of M_w determined by means of SEC−UNICAL. For comparison, the corresponding relaxation times for the linear chains (the lines reproducing the results from Figure 8b) are shown. This allows one to notice that there is a considerable difference in the segmental mobility of the two kinds of systems. It is also reflected in the differences of the glass transition temperatures (compare T_g values in Tables 1 and 2). This effect can be attributed to a much higher concentration of chain ends in the melts of the branched polymers with respect to the melts of linear chains having the same molecular weights. To separate this effect from the macromolecular relaxation rates, the ratio τ_c/τ_s is considered further.

The molecular weight dependences of the normalized chain relaxation times in melts of both (linear and branched) samples are compared in Figure 10. Both can be represented by scaling power laws, but with remarkably different scaling exponents. For the melts of linear chains, the exponent 3.39 is observed close to the typical value of 3.4 for such systems. In contrast, for the fractions of the branched polymer, the exponent is considerably lower (2.61). It is interesting to note that the value of the normalized chain relaxation time for the feed polymer with the broad MWD fits nicely into the data for the fractions with narrow MWDs. This seems to indicate that conclusions can also be drawn from a series of hyperbranched polymers with broad MWDs.

The difference in the scaling exponents for the melts of linear and branched molecules indicates differences in their relaxation mechanisms. The relaxation in the melts of linear polymers is considered to be mainly influenced by entanglements. In the melts of highly branched polymers, it can be supposed that the entanglements have negligible meaning because of the strongly limited possibility of interpenetration between neighboring molecules. The relatively high branching density leads to a compact structure of individual macromolecules; however, they are probably highly deformable. In addition, the high concentration of chain ends might preferentially fill the intermolecular areas and make a flow consisting of intermolecular slippage possible. The rates of rearrangements according to such a mechanism should strongly depend on the branching density, and further investigations in which this parameter is varied can help to explain the reported behavior better.

Some information concerning the intramolecular relaxation of the hyperbranched polymers can be obtained from an analysis of the viscoelastic characteristics within the range between the segmental and the terminal relaxation times. In contrast to the behavior of melts with linear chains, in the case of hyperbranched polymers, the range between the distinguished local and terminal relaxations can be characterized by the values of G' and G'' changing nearly in parallel and by the viscosity variation having a frequency with a considerably different exponent α_{vs}. This can be considered as an indication of the extremely broad spectrum of internal relaxations in these macromolecules. To illustrate this effect, the frequency dependences of the complex viscosities for both linear and hyperbranched polymer melts are compared in Figure 11. The exponents determined for the longest linear chains and for the fraction of hyperbranched polymers with the highest molecular mass are indicated in the figure. The value of $\alpha_{vs} \approx -0.54$ obtained for the hyperbranched melt strongly resembles the behavior of the microgels prepared by Antonietti et al.[39] and of the near-critical gels for which Winter et al.[40,41] found a scaling exponent of $\alpha_{vs} = -0.5$.

Conclusions

Viscosity properties in solution and in the melt of highly branched poly(methyl methacrylate) lead to scaling exponents that are considerably lower than those for linear PMMA. In solution, the intrinsic viscos-

ity of the branched polymer scales with the molecular weight with a Mark−Houwink exponent of $\alpha = 0.40$ (for linear PMMA, $\alpha = 0.688$). The corresponding scaling exponent of the normalized chain relaxation times is 2.61, considerably lower than that for linear PMMA (3.39), because of the absence of entanglements. The complex melt viscosity depends on the frequency with an exponent $\alpha_{vs} \approx -0.54$, which is close to the value found for microgels and near-critical gels.

Acknowledgment. This work was supported by the Deutsche Forschungsgemeinschaft within Sonderforschungsbereich 262. The authors are indebted to the group of Prof. Dr. H. Ritter, Universität Mainz, for lending their preparative SEC columns. P.S. thanks Dr. Daniela Held, Mainz, for helpful discussions concerning GPC measurements.

References and Notes

(1) Fréchet, J. M. J.; Henmi, M.; Gitsov, I.; Aoshima, S.; Leduc, M. R.; Grubbs, R. B. *Science* **1995**, *269*, 1080.
(2) Müller, A. H. E.; Yan, D.; Wulkow, M. *Macromolecules* **1997**, *30*, 7015.
(3) Aoshima, S.; Fréchet, J. M. J.; Grubbs, R. B.; Henmi, M.; Leduc, L. *Polym. Prepr. (Am. Chem. Soc., Div. Polym. Chem.)* **1995**, *36*, 531.
(4) Gaynor, S. G.; Edelman, S.; Matyjaszewski, K. *Macromolecules* **1996**, *29*, 1079.
(5) Hawker, C. J.; Fréchet, J. M. J.; Grubbs, R. B.; Dao, J. *J. Am. Chem. Soc.* **1995**, *117*, 10763−10764.
(6) Sunder, A.; Hanselmann, R.; Frey, H.; Mülhaupt, R. *Macromolecules* **1999**, *32*, 4240.
(7) Simon, P. F. W. Diplomarbeit, Universität Mainz, Mainz, Germany, 1996.
(8) Simon, P. F. W.; Radke, W.; Müller, A. H. E. *Polym. Prepr. (Am. Chem. Soc., Div. Polym. Chem.)* **1997**, *38* (1), 498.
(9) Simon, P. F. W.; Radke, W.; Müller, A. H. E. *Makromol. Chem., Rapid Commun.* **1997**, *18*, 865.
(10) Sakamoto, K.; Aimiya, T.; Kira, M. *Chem. Lett.* **1997**, 1245.
(11) Fréchet, J. M. J.; Aoshima, S. (Cornell Research Foundation, Inc.). U.S. Patent 5,663,260; *Chem. Abstr.* **1997**, *125*, 87505q.
(12) Litvinenko, G. I.; Simon, P. F. W.; Müller, A. H. E. *Macromolecules* **1999**, *32*, 2410.
(13) Litvinenko, G. I.; Simon, P. F. W.; Müller, A. H. E. *Macromolecules* **2001**, *34*, in press.
(14) Hanselmann, R.; Hölter, D.; Frey, H. *Macromolecules* **1998**, *31*, 3790.
(15) Sunder, A.; Frey, H.; Mülhaupt, R. *Polym. Mater. Sci. Eng.* **1999**, *80* (1), 203.
(16) Simon, P. F. W. Dissertation, Universität Mainz, Mainz, Germany, 2000.
(17) Cheng, G.; Simon, P. F. W.; Hartenstein, M.; Müller, A. H. E. *Macromol. Rapid Commun.* **2000**, *21*, 846.
(18) Burchard, W. *Adv. Polym. Sci.* **1999**, *143*, 113.
(19) Nunez, C. M.; Chiou, B. S.; Andrady, A. L.; Khan, S. A. *Macromolecules* **2000**, *33*, 1720.
(20) Sendijarevic, I.; McHugh, A. *Macromolecules* **2000**, *33*, 590.
(21) Jackson, C.; Chen, Y.-J.; Mays, J. W. *J. Appl. Polym. Sci.* **1996**, *59*, 179.
(22) Wyatt, P. J. *Anal. Chim. Acta* **1993**, *272*, 1.
(23) Wyatt, P. J. *J. Chromatogr. A* **1993**, *648*, 27.
(24) Grubisic, Z.; Rempp, P.; Benoît, H. *J. Polym. Sci. B* **1967**, *5*, 755.
(25) Dicker, I. B.; Hertler, W. R.; Cohen, G. M.; Farnham, W. B.; Del Laganis, E.; Sogah, D. Y. *Polym. Prepr. (Am. Chem. Soc., Div. Polym. Chem.)* **1987**, *28* (1), 106.
(26) Ojima, I.; Kumagai, M. *J. Organomet. Chem.* **1976**, *111*, 43.
(27) Müller, M. A.; Stickler, M. *Makromol. Chem., Rapid Commun.* **1986**, *7*, 575.
(28) Müller, A. H. E. *Makromol. Chem., Macromol. Symp.* **1990**, *32*, 87.
(29) Simon, P. F. W.; Müller, A. H. E., manuscript submitted to *Macromolecules*.
(30) Webster, O. W.; Hertler, W. R.; Sogah, D. Y.; Farnham, W. B.; RajanBabu, T. V. *J. Macromol. Sci., Chem.* **1984**, *A21*, 943.
(31) Dicker, I. B.; Cohen, G. M.; Farnham, W. B.; Hertler, W. R.; Laganis, E. D.; Sogah, D. Y. *Macromolecules* **1990**, *23*, 4034.
(32) Brittain, W. J.; Dicker, I. B. *Macromolecules* **1989**, *22*, 1054.
(33) Benoît, H.; Grubisic, Z.; Rempp, P.; Decker, D.; Zilliox, J. G. *J. Chem. Phys.* **1966**, *63*, 1507.
(34) Hobson, L. J.; Feast, W. J. *Chem. Commun.* **1997**, 2067.
(35) Maier, G.; Zech, C.; Voit, B.; Komber, H. *Macromol. Chem. Phys.* **1998**, *199*, 2655.
(36) Stickler, M. Dissertation, Universität Mainz, Mainz, Germany, 1977.
(37) Zammit, M. D.; Davis, T. D. *Polymer* **1997**, *38*, 4455.
(38) Stockmeyer, W. H.; Fixman, M. *Ann. N.Y. Acad. Sci.* **1953**, *57*, 334.
(39) Antonietti, M.; Rosenauer, C. *Macromolecules* **1991**, *24*, 3434.
(40) Chambon, F.; Pertrovic, Z. S.; MacKnight, W. J.; Winter, H. H. *Macromolecules* **1986**, *19*, 2146.
(41) Muthukumar, M.; Winter, H. H. *Macromolecules* **1986**, *19*, 9.

MA0014766